Experimental Investigation of the Aerodynamics of a Modeled Dragonfly Wing Section

Michelle Kwok* and Rajat Mittal †
Department of Mechanical and Aerospace Engineering
The George Washington University
Washington DC 20052
U.S.A

It has been shown in previous studies (Kessel 2000, Vargas & Mittal 2004) that at low Reynolds numbers, a pleated wing section of the type found in dragonflies can generate more lift than a profiled wing with the same cross-section. The focus of the current research project is to further investigate the aerodynamics of pleated wing-sections using experiments. The objective is to understand the flow around a pleated wing and to provide explanations of how the flow pattern corresponds to the lift and drag measurements. Experiments have been conducted using both a wind tunnel and a water channel. In addition to the pleated wing, we have also investigated a "profiled" airfoil which is a smoothened version of the pleated foil. The wind tunnel was equipped with a force balance which allows us to measure the lift and drag on the airfoil sections. The flow around the model was visualized through a dye injection methodology in the water channel. Different flow patterns at various angles of attack were observed and images were captured. The wind tunnel measurements show that the presence of the pleats does marginally improve the lift-drag characteristics of the airfoil and the water channel visualizations provide a clear view of the complex flow structures that form inside the pleats.

Nomenclature

α	=	Angle of attack
C_l	=	Lift coefficient
C_d	=	Drag coefficient
Re	=	Reynolds number
t	=	Time
C	=	Chord
OD	=	Diameter of tube

I. Introduction

Through evolutionary change and other means of adaptation, insect species have to be able to survive under unpredictable environmental conditions. One of the special qualities of insects is their superlative capability of flight. With the advent of micro-aerial vehicles, it has become clear that there is much that can be learnt from insect

* Undergraduate student (Senior), Department of Mechanical and Aerospace Engineering, 2030 F ST N.W., Apartment 906, Washington D.C. 20006, AIAA Student Member.
† Associate Professor, Department of Mechanical and Aerospace Engineering, Suite T729, 801 22 nd Street N.W., Academic Center, Washington, D.C. 20052, AIAA Senior Member.

flight that could be translated into engineered systems. It is this reason that makes further investigation into the aerodynamic aspect of an insect wing worthwhile. This study focuses on the aerodynamic characteristics and the flow pattern around a dragonfly wing of a particular cross-section.

Dragonfly wings are complex in structure, composed of interesting wing cross-sections that are pleated and vary across the wing chord. The pleated profile and the distinct composition are reinforcements to the wing structure to enhance the flight performance in several ways. The pleated network handles the spanwise bending [1] force while the vein arrangements (figure 1) preclude mechanical wear that the wing experiences during flapping. Veins can be divided into three sub-categories- longitudinal, cross and secondary. The front of fore and hind wings have longitudinal veins that run almost parallel to the leading edge along the span of the wing. Along the longitudinal veins, there exist cross veins where finer networks of secondary veins extend from it, finishing a dragonfly wing's physical structure. The main function of these vein arrangements is to stiffen the thin membranous wing so that the insect can withstand the inertia forces that act on it. The cross veins allow the wing to transform its shear forces to tension forces. While the secondary veins seem to be a minor structure, it helps maintain structural integrity as well as provide stability effects. [2]

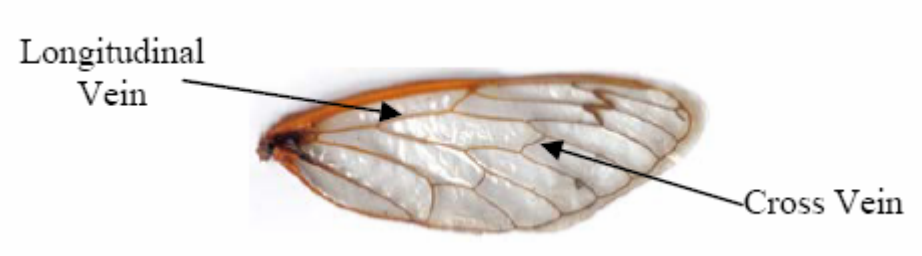

Figure 1. Vein arrangement of a Cicada

The notion that a pleated airfoil posses poor aerodynamics performance seems at first glance to be an obvious conclusion. After all, it is the shape and smoothness of a traditional airfoil that allows today's aircrafts to fly. However, the conclusion that a pleated wing has poor aerodynamic performance flies in the face of evolution since it is unlikely that after millions of years of evolution, insects such as dragonflies are saddled with poorly performing wings. Previous experimental results on dragonfly wings in steady flow have led to some unexpected findings. It was found that at low Reynolds numbers, the pleated dragonfly wing generates comparable and even higher lift relative to a conventional smooth airfoil. There were several attempts[1] to explain this observation. One explanation is that air flowing over the wing pleats become stagnant or rotates slowly and essentially creates a virtual streamline foil shapel[4]. Another explanation is that as the angle of attack increases, flow starts to separate from the leading edge and a separation bubble is formed that due to the interaction with the pleats, reattaches sooner than for a corresponding smooth airfoil[1].

Experimental measurements of the aerodynamic characteristics of different dragonfly wing cross-sections were taken by Kesel[3] and a computational study corresponding to the same configuration has been undertaken by Vargas and Mittal[1]. In the current study, we have use both wind-tunnel force measurements and water channel flow visualizations to further examine the aerodynamic characteristics of these foils. The wind tunnel is equipped with a force balance that allows us to measure the lift and drag of the selected dragonfly cross-section (figure 2)[3]. The flow pattern around the wing was also studied by the use of a water channel and a dye injection mechanism. It is hoped that the interpretation of the flow pattern images taken would enhance the level of understanding behind the aerodynamic characteristics of a dragonfly wing.

a) **b)**

Figure 2. Selected cross-section of a dragonfly wing a) pleated airfoil b) profiled airfoil

II. Wind Tunnel and Water Channel Methodology

A dragonfly wing with an approximate cross-section as shown in figure 2 was machined. The model was made of a piece of 0.2mm thick aluminum sheet. It has an 8" chord and 14" span. The profiled airfoil was obtained by wrapping transparent tape around the pleated aluminum model. Both sets of experiments were conducted at low Reynolds numbers so that results are comparable.

A. Lift and Drag Measurements:

The wind tunnel (figure 3) used has a 14" by 10" test section. Air is induced through the tunnel by suction. A honeycomb and two screens are located ahead of the contraction to provide uniform low turbulence flow. An adjustable speed ranging from 5 mph up to 150 mph can be selected. The speed is controlled manually through a vane system, which changes the angle at which the air enters the rotor.

The airfoil is mounted on the wind tunnel force balance where the angle of attack is controlled through a knob. The balance is of the pyramidal type and can be used to measure lift and drag forces. The lift and drag components are separated by mechanical linkage and component readings are provided in the electrical output. The individual components are measured by strain gauge load cells. In order to obtain the lift and drag measurement of the airfoil, the balance was calibrated to obtain the relationship between the electrical output of the load cells (measured in millivolts), and the applied lift and drag force (measured in Newtons). This was done by applying a series of known forces in the vertical and horizontal directions using pulley mechanisms. This process generates a graph that gives the relationship between the output force in Newtons and millivolts, which can be used later to find the lift and drag force in Newtons by matching up with the corresponding millivolts readings obtained.

Upon the completion of calibrating the force balance, wind tunnel tests can be conducted. Velocity was set at 5 mph which corresponds to Re ≈ 31200. Lift and drag load cell outputs were recorded for a range of angle of attack from α=-15˚ to α=15˚ at increments of 5 degrees. Finally, outputs in millivolts are converted into Newtons by using the calibration curve.

Figure 3. Test section and pyramidal force balance of the wind tunnel

B. Flow Visualization Technique:

The water channel (figure 4) which has clear acrylic walls is 24" wide with water depth variable up to 12". The water speed is variable and controlled by changing the pressure of the water pump. The injection fluid is composed of ink and alcohol. The ink is the primary component of the mixture, with small proportion of alcohol added to lower the density of the mixture and make it comparable to the density of water. This mixture is introduced via a tube with 0.04 and 0.060" OD at exit. Tests were conducted with the same wing cross-section from α=-15 to α=15 at

increments of 5 degrees and still images were captured during the experiment. The set of experiments was conducted with a water freestream velocity of 0.01451 m/s which corresponds to Re ≈ 2255. This lower velocity allows us to capture clear images and the low Reynolds number is also commensurate with small insects and micro-aerial vehicles.

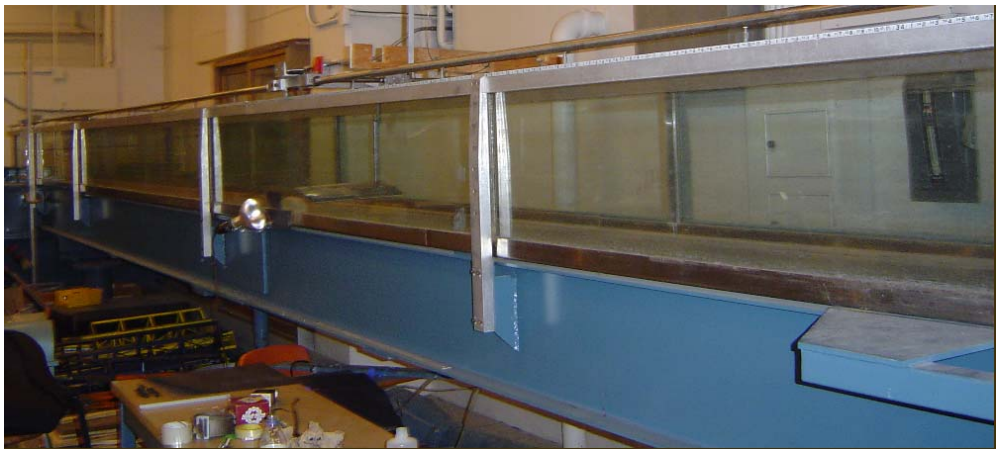

Figure 4. Water channel

III. Results

The following sections discuss the lift and drag forces of the pleated and profiled airfoil obtained from the wind tunnel experiments. Following this is a presentation of the flow visualization around both airfoils. Images are shown at different angle of attack where flow patterns are discussed and compared to the corresponding lift and drag measurements for relevancy.

The lift and drag coefficients curves and drag polar for the pleated airfoil and the profiled airfoil are shown in figure 5. It was found from figure 5a that the lift coefficient of the profiled airfoil is higher than the pleated airfoil at negative angles of attack. Since the aerodynamic performance at negative angles of attack is of less importance, not being able to produce as much lift at these angles of attack would not be a significant disadvantage. At positive angles of attack, the lift coefficient values were comparable. In fact, at $\alpha = 10^{\circ}$ angle of attack, the lift coefficients for the two foils were exactly the same. Figure 5b also reveals that the drag coefficient of the profiled airfoil is higher than the pleated airfoil for most of the data points. This seems surprising at first glance since the profiled airfoil seems much more streamlined than the pleated airfoil. But as explained by Vargas and Mittal[1], the reason for this is due to the reverse flow inside the pleats, the pleated airfoil experiences lower skin-friction drag which at these low Reynolds number is a not a insignificant contributor to the total drag. Figure 5c is a representation of the relationship between the lift and drag coefficients. Focusing on the positive angle of attack portion of the plot, it is shown that when both airfoils have the same lift coefficient of 0.14, the pleated airfoil has a lower drag compared to the profiled airfoil. This concludes that the aerodynamic performance of the pleated airfoil is comparable and even marginally better than the profiled airfoil because it provides less drag force.

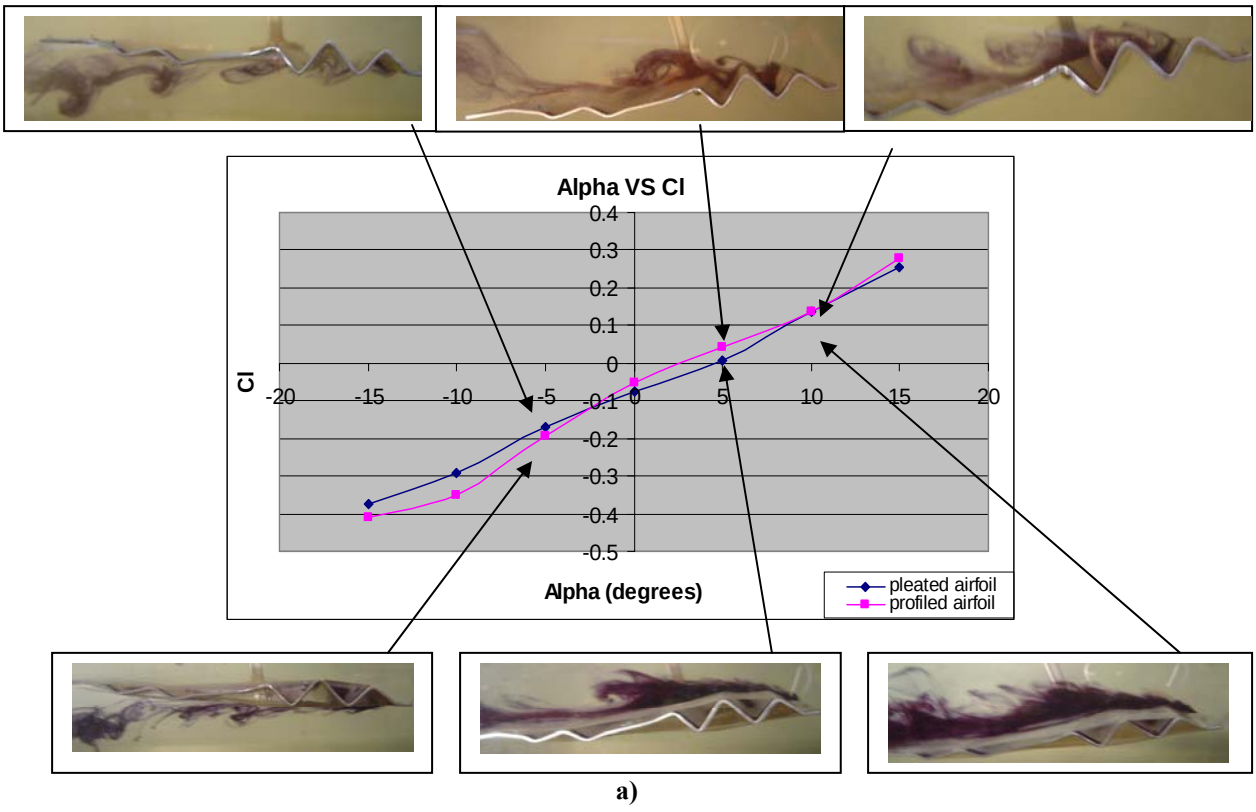

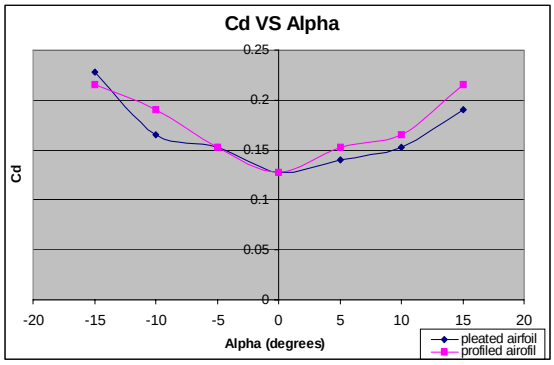

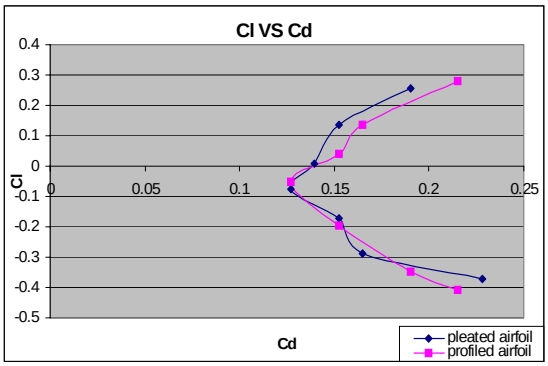

Figure 5. Aerodynamic performance of the pleated and profiled airfoils a) lift coefficient b) drag coefficient c) drag polar curve

Flow visualization images showing the location of flow separation, flow reattachment and vortices in the pleats are shown in figure 6. This image was captured at an angle of attack of 0˚ and the first fold of the pleated airfoil is in focus in figure 6a. The onset of flow separation occurred at the beginning of the first fold and as it reaches the end of the fold, it wraps around to form a vortex. Finally, as the vortex convects out of the fold, the flow reattaches itself where a second vortex is formed in the second fold and so on.

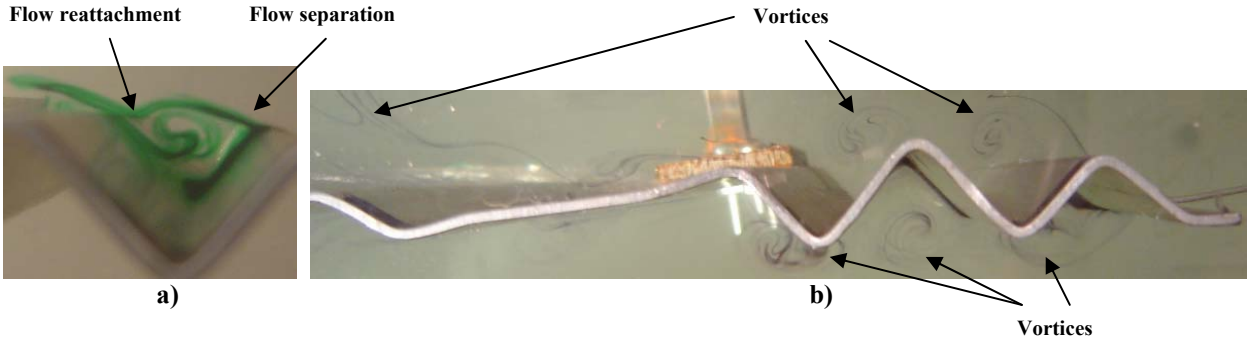

Figure 6. Flow pattern of the pleated airfoil a) first fold b) full airfoil at α= 0˚ angle of attack

Flow patterns around the airfoils at α= 15˚ angle of attack are also shown. Images were captured at three different time instances for both the pleated and profiled airfoils so that the vortices' path can be traced. The arrangement of the images in figure 7 allows one to make easy comparisons of the flow pattern for each airfoil at a specific time. These images clearly describe the flow separation and reattachment processes with respect to time for the pleated airfoil. For the profiled airfoil the onset of vortices formation was visualized at the root chord. Tiny vortices were observed up to ½C where larger vortices and turbulent flow dominates along the rest of the wing chord.

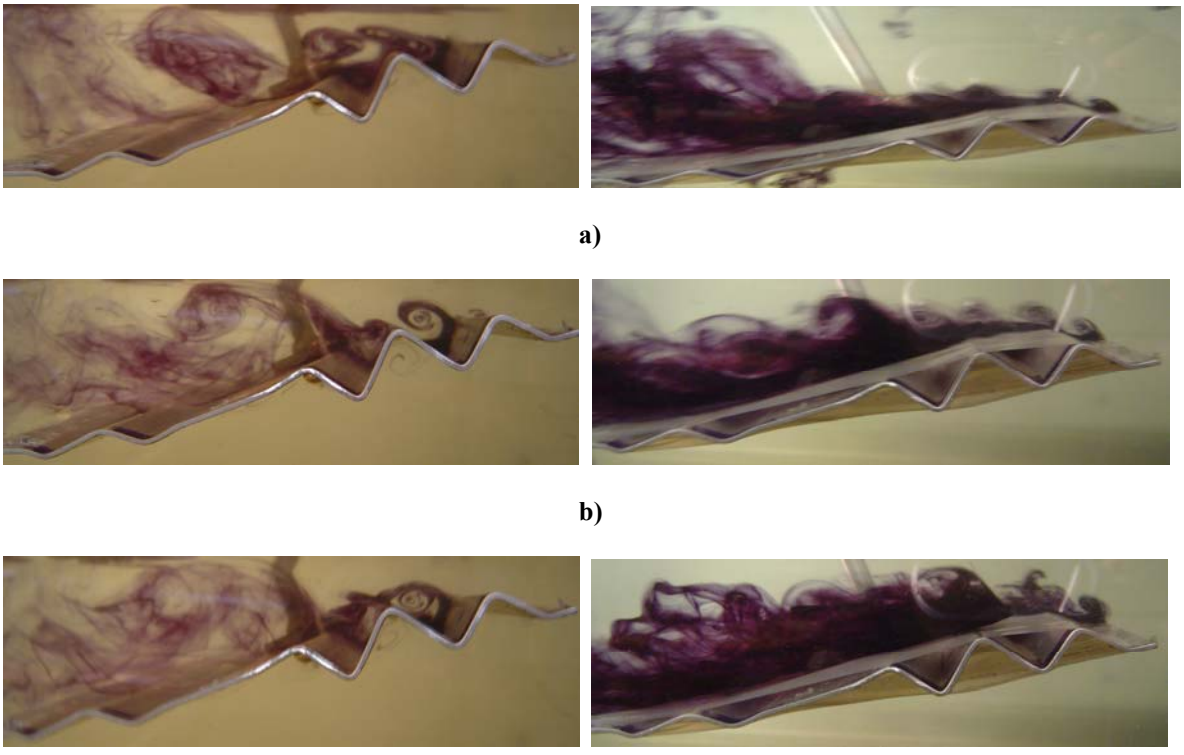

a)

b)

c)

Figure 7. Flow patterns of the pleated and profiled airfoils a) t1 b) t2 c) t3 where t3> t2> t1 at α= 15˚ angle of attack (right column- profiled airfoil and left column- pleated airfoil)

IV. Conclusions

A flow visualization technique has been used to understand the flow behavior around a pleated and a profiled dragonfly cross-section as shown in figure 2. A comparison between the flow behavior around the two airfoils was made and an explanation of the flow patterns and how it corresponds to the lift and drag measurements has been provided. The lift coefficient for the profiled airfoil is higher than the pleated airfoil at a negative angle-of-attack range of $-15^\circ \leq \alpha < 2.5^\circ$. Since the aerodynamic performance at negative angle of attack is of less importance, the pleated airfoil is not at a significant disadvantage. At positive angles of attack, the differences are small and the results are comparable. The drag coefficients for the selected range of angle of attack show that the pleated airfoil produces less or exactly the same amount of drag when compared to the profiled airfoil, except at $\alpha = -15^\circ$ angle of attack. This confirms that the overall aerodynamic performance of a pleated wing is at least comparable to and sometimes better than a profiled wing and this is consistent with Kesel's[3] finding. The aerodynamic performance in the pleated structure can be explained by the reverse flow in the folds, which leads to a lower skin friction drag. It should be pointed out that the wind tunnel experiments could not be conducted at Reynolds numbers lower than about 30,000 due to the limitations in the speed imposed by the wind-tunnel. In the future we expect to make force measurements at Reynolds number less than 10,000 and these will allow for a clearer comparison between the water tunnel visualization and the wind tunnel measurements.

Acknowledgements

The authors would like to acknowledge the assistance of Zaak Beekman, a sophomore mechanical engineering student at the George Washington University.

References

[1] Vargas, A. and Mittal, R. "Aerodynamic Performance of Biological Airfoils," AIAA 2004-2319, 2nd Flow Control Conference, Portland, Oregon, 2004.

[2] Kesel, A. B., Philippi, U. and Nachtigall, W., "Biomechanical Aspects of Insect Wings – An Analysis using the Finite Element Method," *Computers in Biology and Medicine,* Vol. 28, 1998, pp. 423–437.

[3] Kesel, A. B., "Aerodynamic Characteristics of Dragonfly Wing Sections Compared with Technical Aerofoil," *Journal of* Experimental Biology, Vol. 203, 2000, pp. 3125-3135.

[4] Rees, C. J. C., "Aerodynamic Properties of an Insect Wing Section and a Smooth Aerofoil Compared," *Nature*, Vol. 258,13 Nov. 1975b, pp 141-142.